EPJ Web of Conferences **86**, 00016 (2015)
DOI: 10.1051/epjconf/ 20158600016

Fission dynamics of $^{240}Cf^{*}$ formed in $^{34,36}S$ induced reactions

Deepika Jain, Gurvinder Kaur and Manoj K. Sharma[a]

School of Physics and Materials Science, Thapar University, Patiala-147004, India

Abstract. We have studied the entrance channel effects in the decay of Compound nucleus $^{240}Cf^{*}$ formed in $^{34}S+^{206}Pb$ and $^{36}S+^{204}Pb$ reactions by using energy density dependent nuclear proximity potential in the framework of dynamical cluster-decay model (DCM). At different excitation energies, the fragmentation potential and preformation probability of decaying fragments are almost identical for both the entrance channels, which seem to suggest that decay is independent of its formation and entrance channel excitation energy. It is also observed that, with inclusion of deformation effects upto quadrupole within the optimum orientation approach, the fragmentation path governing potential energy surfaces gets modified significantly. Beside this, the fission mass distribution of Cf* isotopes is also investigated. The calculated fission cross-sections using SIII force for both the channels find nice agreement with the available experimental data for deformed choice of fragments, except at higher energies. In addition to this, the comparative analysis with Blocki based nuclear attraction is also worked out. It is observed that Blocki proximity potential accounts well for the CN decay at all energies whereas the use of EDF based nuclear potential suggests the presence of some non-compound nucleus process (such as quasi-fission (qf)) at higher energies.

1 Introduction

The concept of Bohr hypothesis [1] presumes that the excitation process leaves the nucleus in a sufficiently complex state so that the subsequent decay is independent of formation process, except for the requirement of various conservation laws. The theoretical implementation of this hypothesis has been quite successful in describing a large amount of experimental data governing the decay of compound nuclei formed in heavy-ion fusion reactions [2]. In such reactions, the Compound nucleus (CN) is formed at a particular excitation energy with a broad range of angular momentum from $\ell=0\hbar$ to ℓ_{max}. Depending upon the incident energy of the projectile as well as angular momentum, the collision of interacting nuclei may lead to several interesting phenomena such as particle production, quasifission (qf), incomplete fusion (ICF) etc., in addition to the usual complete fusion (CF) process. The heavy ion collisions at low energies generally lead to CF process, involving the total amalgamation of the colliding nuclei forming an equilibrated compound nucleus. However, in certain cases, the composite system formed by the projectile and target nuclei may reseparate before complete fusion leading to some non compound nucleus process such as quasi-fission (qf). Many factors, such as deformation and orientation of the colliding nuclei, their mass asymmetry and the closed shell structure etc., may potentially affect the qf process. Thus the choices of a suitable projectile-target combination as well as optimum beam energy are crucial for a successful synthesis of the heavy nuclei.

Recently, an experiment was performed to measure fission cross section of $^{240}Cf^{*}$ produced in irradiation of $^{204,206}Pb$ target with $^{36,34}S$ ions respectively at energies above as well as below the Coulomb barrier [3]. It is of interest to study $^{240}Cf^{*}$ system as it is formed via two different incoming channels and belongs to actinide region whose experimental data on decay properties are rare due to low production rate.

Here, we study the decay of compound nucleus $^{240}Cf^{*}$ by using the dynamical cluster decay model (DCM) [4,5] via the nuclear proximity potential derived from Skyrme energy density formalism (SEDF) [6,7] having an advantage of using different Skyrme forces with different barrier characteristics. It is worth mentioning that DCM treats all the decay processes (ER, fission and qf) on equal footing as barrier penetration of preformed fragments [8]. The DCM is the extension of preformed cluster model (PCM) [9] used by Gupta and collaborators [10] to calculate the α-decay half-life time for $^{249,252}Cf$, which find nice agreement with experimental data. Moreover, they also predicted some probable heavy clusters from both the parent nuclei.

In the present paper, firstly the role of deformations upto quadrupole moment is analysed in decay of neutron deficient nucleus $^{240}Cf^{*}$ formed using two different incoming channels in framework of DCM. It is observed that with the inclusion of deformation and optimum orientation [11] effects, the fission distribution changes and α-nucleus structure starts appearing. We have used

[a] msharma@thapar.edu

well established SIII force to study the entrance channel effects through fragmentation potential and preformation probability distribution. The fragmentation potential is plotted as a function of light fragment mass A_2 varying from A_2=1 to A_{CN} /2. The complementary fragments (A_1 =A_{CN} - A_2) vary as a mirror image and are not considered for the case of simplicity. However, to have an idea of relative preformation of all fragments, the preformation probability P_0 is plotted over entire mass region A_i (i=1,2). It is important to mention here that by using SIII force, the decay process of $^{240}Cf^*$ nucleus formed at different entrance channel excitation energy, seems independent of the entrance channel effects. Besides this, the effect of adding two neutrons in the target is seen by studying the decay of Cf^* isotopes. The fission cross sections are fitted by using SIII force in SEDF as well as via Blocki potential [12]. Although, Blocki based nuclear interaction fits the data over entire range of incident energies, the SEDF based nuclear proximity seems to suggest some competing mechanism such as quasi-fission (qf) at higher energies.

2 The Methodology

2.1 The dynamical cluster-decay model (DCM)

The DCM [4,5,13,14] is worked out in terms of the collective coordinates of mass (and charge) asymmetries: $\eta = (A_1 - A_2) / (A_1 + A_2)$ [and $\eta_Z = (Z_1 - Z_2) / (Z_1 + Z_2)$, where 1,2 stands for heavy and light mass fragments], relative separation R, the multipole deformations $\beta_{\lambda i}$, and the orientations θ_i (i=1,2) of two nuclei in the same plane. We define the decay cross-sections in terms of the partial wave analysis as:

$$\sigma = \frac{\Pi}{k^2}\sum_{\ell=0}^{\ell_{max}}(2\ell+1)P_0^{\ell}P_{\ell}, k = \sqrt{\frac{2\mu E_{c.m.}}{\hbar^2}} \quad (1)$$

where P_0, the preformation probability refers to η motion and P, the penetrability refers to R motion. The maximum angular momentum, ℓ_{max} is related to the decay channel and is defined at a pont where light particle cross-sections are negligible, $\sigma_{LP} \rightarrow 0$.

P_0 for each ℓ is the solution of the stationary Schrodinger equation in η, at a fixed R,

$$\left\{-\frac{\hbar^2}{2\sqrt{B_{\eta\eta}}}\frac{\partial}{\partial\eta}\frac{1}{\sqrt{B_{\eta\eta}}}\frac{\partial}{\partial\eta}+V_R(\eta,T)\right\}\psi^{\nu}(\eta)=E^{\nu}\psi^{\nu}(\eta) \quad (2)$$

and the penetrability is calculated by WKB integral. The deformation and orientation dependent fragmentation potential in Eq. (2), at given temperature (T), is given by

$$V_R(\eta,T)=\sum_{i=1}^{2}[V_{LDM}(A_i,Z_i,T)]+\sum_{i=1}^{2}[\delta U_i]\exp(-T^2/T_0^2)+V_c(R,Z_i,\beta_{\lambda i},\theta_i,T)$$
$$+V_N(R,A_i,\beta_{\lambda i},\theta_i,T)+V_\ell(R,A_i,\beta_{\lambda i},\theta_i,T) \quad (3)$$

For details of fragmentation potential and T-dependence refer [4]. Besides using Blocki interaction [12], we have used here the skyrme energy density dependent proximity potential, and the same is discussed in brief in section 2.2

2.2 SEDF based proximity potential within Extended Thomas Fermi (ETF) approach

The nucleus-nucleus interaction potential in SEDF based on semiclassical ETF model, is

$$V_N(R) = E(R) - E(\infty) \quad (4)$$

i.e. the nucleus-nucleus interaction potential as a function of separation distance, $V_N(R)$, is the difference of the energy expectation value E of the colliding nuclei that are overlapping (at a finite separation distance R) and are completely separated (at R=∞),where

$$E = \int H(\mathbf{r})d\mathbf{r} \quad (5)$$

with Skyrme Hamiltonian density taken from Ref. [18].

The Skyrme force parameters, used in the Hamiltonian were fitted by different authors to obtain better descriptions of various ground state properties of nuclei. Densities of compound nucleus are added under frozen density approximation, defined as:

$$\tau(\rho)=\tau_1(\rho_1)+\tau_2(\rho_2), \qquad \mathbf{J}(\rho)=\mathbf{J_1}(\rho_1)+\mathbf{J_2}(\rho_2) \quad (6)$$

with $\rho_i=\rho_{in}+\rho_{ip}$, $\tau_i(\rho_i)=\tau_{in}(\rho_{in})+\tau_{ip}(\rho_{ip})$, $\mathbf{J_i}(\rho_i)=\mathbf{J_{in}}(\rho_{in})+\mathbf{J_{ip}}(\rho_{ip})$. Here ρ_q, τ_q and J_q (q=n,p) are the nucleonic, kinetic energy and spin-orbit densities, respectively. For nuclear density ρ_i, we used the T-dependent Fermi density distribution

$$\rho_i(z_i)=\rho_{oi}(T)\left[1+\exp\left(\frac{z_i-R_i(T)}{a_i(T)}\right)\right]^{-1} \quad (7)$$

with z_2 = R-z_1 = [$R_1(\alpha_1)+R_2(\alpha_2)$+s] − z_1, where z_1, z_1 are radius vector along collision axis , R_1, R_2 are radius of fragments A_1, A_2 respectively, α_1, α_2 are angles that radius vector $R_i(\alpha_1)$ of the colliding nuclei makes with symmetry axis and s is the minimum separation distance. The central density

$$\rho_{0i}(T)=\frac{3A_i}{4\pi R_i^3(T)}\left[1+\frac{\pi^2 a_i^2(T)}{R_i^2(T)}\right]^{-1}$$

with nucleon densities ρ_{iq} further defined as $\rho_{in}=\frac{N_i}{A_i}\rho_i$, $\rho_{ip}=\frac{Z_i}{A_i}\rho_i$, and the half density radii R_{0i} (T =0) and the surface thickness parameters a_i(T = 0) obtained by fitting the experimental data to the polynomials in nuclear mass A (= 4–238), as [15]

$$R_{0i}\,(T=0) = 0.9543+0.0994A_i-9.8851\text{x}10^{-4}A_i^2$$
$$+4.8399\times10^{-6}A_i^3-8.4366\times10^{-9}A_i^4,$$
$$a_i\,(T=0) = 0.3719+0.0086A_i-1.1898\times10^{-4}A_i^2 \quad (8)$$
$$+6.1678\times10^{-7}A_i^3-1.0721\times10^{-9}A_i^4$$

The temperature dependence in the above formulae are introduced in reference to [16]

$$R_{0i}(T)=R_{0i}(T=0)[1+0.0005T^2], \quad (9)$$
$$a_i(T)=a_i(T=0)[1+0.01T^2]$$

The radius vector $R_i(\alpha_i)$ is related to nuclear radii R_{0i} as

$$R_i(\alpha_i,T)=R_{0i}(T)[1+\sum_{\lambda}\beta_{\lambda i}Y_{\lambda}^{0}(\alpha_i)] \quad (10)$$

3 Calculations and Results

Firstly, we study the variation of fragmentation potential V(η) for the decay of CN $^{240}Cf^*$ formed in $^{34}S+^{206}Pb$ and $^{36}S+^{204}Pb$ reactions at $E_{c.m.}$ ~138 MeV, at the extreme values of angular momentum i.e., at $\ell = 0\ \hbar$ and ℓ_{max}, with spherical and deformed choice of decaying nuclei as shown in Fig. 1 (a) and (b) respectively. At $\ell = 0\hbar$, the fragmentation profile is quite similar but at $\ell = \ell_{max,}$ the

structure of potential energy surface change significantly particularly for Heavy Mass Fragments (HMFs) and fission region with the inclusion of deformation and optimum orientations. In other words, α-nucleus structure starts appearing in the HMF and fission region when deformations are taken into account. Also at $\ell = 0\hbar$, the contribution of the ER is more prominent than the symmetric or asymmetric fission fragments, while the fission fragments start competing with ER process at higher ℓ values. Although, at $\ell=\ell_{max}$ the fission fragment distribution seems near symmetric for spherical as well as deformed fragmentation, however the relative contribution of asymmetric component is higher in case of spherical approach. This means that, in addition to the angular momentum ℓ, deformation and orientations also play an important role in the decay of $^{240}Cf^{*}$ nucleus formed via $^{34,36}S$ induced reactions.

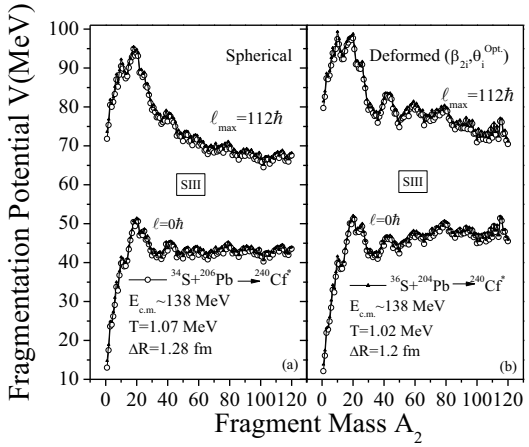

Figure 1. Fragmentation potential for the decay of $^{240}Cf^{*}$ formed in $^{34}S+^{206}Pb$ and $^{36}S+^{204}Pb$ reaction channel at comparable $E_{c.m.}$ values using (a) spherical and (b) deformed nuclei.

After studying the role of angular momentum and deformations, we have studied the entrance channel effect in the decay of $^{240}Cf^{*}$ formed via two different incoming channels. It is also clear from Fig. 1 that the decay of $^{240}Cf^{*}$ is independent of its mode of formation and entrance channel excitation energy both for spherical and deformed choice of nuclei as the decay pattern governed by fragmentation potential seems identical for chosen entrance channels. These results are further clarified in terms of the relative preformation probability P_0, shown in Fig. 2 only for deformed nuclei. Fig.2 shows the preformation probability for the decay of $^{240}Cf^{*}$ at the same ℓ_{max} value and comparable $E_{c.m.}$ values for both the channels. The preformation factors overlap each other (the same fragments are preborn during the decay process) for both the channels, which further seem to suggest that the decay is independent of the choice of entrance channel. One may note here that the contribution of fragments forming secondary peaks (shoulder) is very small (i.e. main contribution is due to the symmetric fragments).

Further, the fission cross-sections for the reaction of ^{36}S beam with $^{204,206,208}Pb$ are available [3]. So, these reactions are worked out to analyse systematics of fission mass distribution with the increase in the isospin (N/Z) ratio of the decaying CN as shown in Fig. 3 (a) at $\ell= \ell_{max}$ value. The calculations are made at $E_{c.m}$ ~138 MeV by taking same ℓ_{max} values (ℓ_{max}=112ħ) and comparable neck-length parameter ΔR, for β_2-deformed fragmentation within optimum orientation approach. The Fig. 3 (a) showing fragmentation potential $V(A_2)$ at $\ell = \ell_{max}$, it is observed that both symmetric as well as asymmetric fission fragments contribute towards the decay of Cf* isotopes, when two or four neutrons are added to $^{240}Cf^{*}$. It is observed that there is not much change in the potential energy surface upto A=90 for all the isotopes of Cf* whereas for A>90, the effective contribution of asymmetric fragments for fission decreases as isospin ratio increases. It is further clarified in Fig. 3(b) which shows the preformation probability only for $90 \le A_i \le 150$ fragments at ℓ_{max} value. It is interesting to notice here that width of asymmetric peak decreases as neutrons are added in $^{240}Cf^{*}$ which seems to indicate that with increase in iso-spin ratio relative contribution of symmetric fragments gets enhanced.

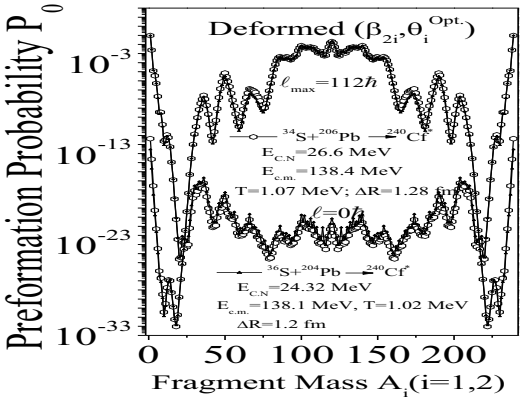

Figure 2. Preformation probability P_0 as a function of fragment mass for the decay of $^{240}Cf^{*}$ formed via two different channels at approximately same $E_{c.m.}$ value using deformed nuclei.

This implies that the addition of two neutrons leads to change in the structure of preformation probability in fissioning region which is in agreement with earlier investigations of Po^{*} isotopes [14].

Table I gives the comparison of experimental data on σ_{fiss} with DCM based calculations for both the incoming channels using SIII force. However, the ER data is not available at reported energies and would be dealt in our future work. From table I, it is clear that the ℓ_{max} values as well as the neck length parameter (ΔR) are of similar order for both the incoming channels, which further indicate that the decay of $^{240}Cf^{*}$ is independent of the entrance channel effect. The cross-sections calculated using DCM are more for ^{36}S induced reaction which is in agreement with experimental observations showing more enhancement for ^{36}S projectile as compared to ^{34}S. However, the DCM calculated σ_{fiss} fits the data nicely at all the reported energies except at one or two higher energies. At these higher energies, some non-compound nucleus component such as qf seem to compete with the fission, and the sum of two i.e. $\sigma_{fiss}+\sigma_{qf}$, fits the available data nicely. Also, the nuclear proximity potential calculated using Blocki formula [12] fits the data even at these highest energies. To look for the possible reason, the preformation probability for the decay of $^{240}Cf^{*}$ using Blocki potential and SIII force at ℓ_{max} value is plotted in Fig.4. It is observed that the structure of preformation

probability changes significantly particularly in HMF and fission region with the use of Blocki potential. Moreover, the fragments that contribute for fission are wider in range for SIII force as compared to Blocki potential. This change in structure seems to influence the CF process at higher incident energies.

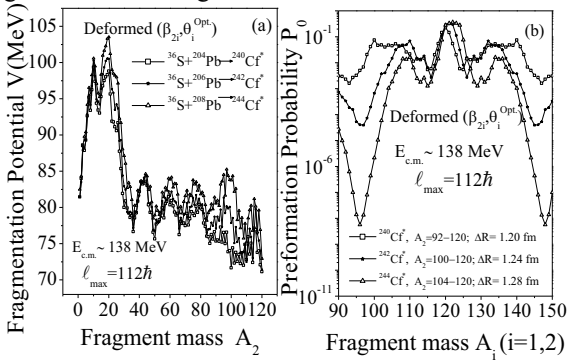

Figure 3. (a) Fragmentation potential and (b) Preformation probability as a function of fragment mass number for $^{240,242,244}Cf^*$ isotopes at $E_{c.m.}$~ 138 MeV.

In conclusion, the decay of $^{240}Cf^*$ formed via two different beams ^{34}S and ^{36}S respectively incident on ^{206}Pb and ^{204}Pb targets, studied using DCM with deformation effects included, is independent of mode of it's formation and entrance channel excitation energy. The entrance channel independence of $^{240}Cf^*$ is also indicated by similar ℓ_{max} values obtained for both the incoming channels. Also the angular momentum and deformation effects are shown to be important in the decay of $^{240}Cf^*$ nucleus. The effect of iso-spin dependence is analysed by studying the decay pattern of different isotopes of Cf^* nucleus. Although Blocki based potential fits the data at all energies, SEDF based SIII force seem to advocate the possibility of qf at higher incident energies. It will be of further interest to study the dynamics of these reactions by employing different Skyrme forces before reaching at definite conclusion regarding emergence of qf component.

Table 1. The fission cross-section for $^{240}Cf^*$ nucleus, calculated by the DCM using SIII force at different $E_{c.m.}$ values, compared with experimental data [3]. 'a' symbolizes qf contribution.

$^{34}S+^{206}Pb \rightarrow ^{240}Cf^*$				
$E_{c.m.}$	ΔR	ℓ_{max}	σ_{fiss} (DCM)	σ_{fiss} (Expt.)
135.3	1.0	107	0.013	0.015
136.7	1.18	110	0.38	0.428
138.4	1.28	112	3.8	3.0
140	1.335	114	9.9	9.36
142.7	1.421	115	34	31.4
146	1.5	115	74	79.3
149.6	1.55	118	153.2	153.6
157.7	1.7	119	340	332
170.4	1.8 1.705[a]	121	302 249[a]	551
$^{36}S+^{204}Pb \rightarrow ^{240}Cf^*$				
135.7	1.04	107	0.026	0.023
137.4	1.08	109	0.054	0.056
138.1	1.2	112	0.85	0.864
139.8	1.31	113	6.8	6.4
142.4	1.41	115	30.8	30.7
145.2	1.463	116	63.2	65.33
148	1.54	117	138.2	138.9
156.6	1.685	118	294	304.2
160.9	1.69 1.615[a]	119	298 75[a]	372.7
169.4	1.72 1.71[a]	121	276 208[a]	484

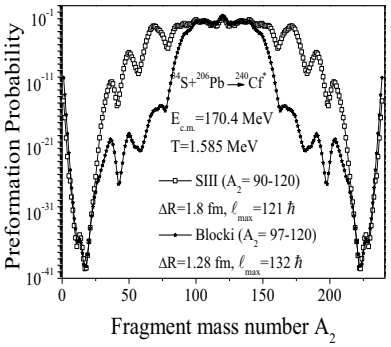

Figure 4. Preformation probability for the decay of CN $^{240}Cf^*$ using SIII force and Blocki interaction potential.

References

1. N. Bohr, Nature (London) **137**, 344 (1936).
2. R. G. Stokstad, *Treatise on Heavy-Ion Science* (Plenum Press, New York) **3**, p. 83 (1985).
3. J. Khuyagbaatar *et al.,* Phys. Rev. C **86**, 064602 (2012).
4. R. K. Gupta, Lecture Notes in Physics **818**, *Clusters in Nuclei*, ed C. Beck, Vol. I, (Springer Verlag) p. 223, (2010) ; B.B. Singh,M. K. Sharma and R. K. Gupta, Phys. Rev. C **77**, 054613 (2008).
5. D. Jain, R. Kumar and M. K. Sharma, Phys. Rev. C **87**, 044612 (2013).
6. J. Bartel and K. Bencheikh, Eur. Phys. J. A **14**, 179 (2002).
7. D. Jain, R. Kumar, M. K. Sharma and R. K. Gupta, Phys. Rev. C **85**, 024615 (2012).
8. M. K. Sharma, S. Kanwar, G. Sawhney, R. K. Gupta and W. Greiner, J. Phys. G : Nucl. Part. Phys. **38**, 055104 (2011).
9. S. S. Malik and R. K. Gupta, Phys. Rev. C **39**, 1992 (1989).
10. M. Balasubramaniam and R. K. Gupta, Phys. Rev. C **60**, 064316 (1999).
11. R. K. Gupta, M. Balasubramaniam, R. Kumar, N. Singh, M. Manhas and W. Greiner, J. Phys. G : Nucl. Part. Phys. **31**, 631 (2005).
12. J. Blocki, J. Randrup, W. J. Swiatecki, and C. F. Tsang, Ann. Phys. (NY) **105**, 427 (1977).
13. G. Sawhney, G. Kaur, M. K. Sharma and R. K. Gupta, Phys. Rev. C **88**, 034603 (2013).
14. M. Kaur and M. K. Sharma, Phys. Rev. C **85**, 054605 (2012).
15. R. K. Gupta, D. Singh, R. Kumar and W. Greiner, J. Phys. G : Nucl. Part. Phys. **36**, 075104 (2009).
16. R. K. Gupta, A. Sandulescu and W. Greiner, Phys. Lett. B **67**, 257 (1977); Rev. Roum. Phys. **23**, 51 (1978).